

Optical Purification of Materials via Electromagnetically Induced Walking

Wenxi Lai*

School of Applied Science, Beijing Information Science and Technology University, Beijing 100192, China

Natural materials are always mixed with impurities or foreign matters, which affect physical or chemical properties of the materials in practice. Here, we give an optical method to purify mixed gaseous atoms. It results from the fact that step length of individual atoms in electromagnetically induced walking depends on their masses and optical transition wave lengths. The optical purification method can be used to separate different chemical elements and isotopes.

PACS numbers: 37.10.Vz, 32.90.+a, 3.75.-b, 42.50.Ct

Material purification is the physical separation of a chemical substance of interest from foreign or contaminating substances. It plays important role in many fields such as medicine, chemistry, manufacturing and current micro-fabrication. Especially the material challenges are limiting urgent progress in frontier technology, for example, quantum computing hardware platforms [1], single photon sources [2], high-temperature superconductivity [3, 4], semiconductor quantum dots [5] and so on. There are many well developed methods of material purification, such as filtration, centrifugation, evaporation, extraction, crystallization, adsorption, smelting, distillation, downstream processing, water purification, fractionation and electrolysis.

In this paper, we propose an optical method of purification based on electromagnetically induced walking (EIW) effect [6]. In EIW, an atom would coherently walk along the direction of propagating light and the velocity of the atom is related to the atom mass and optical transition wave length. This property has potential application in the separation and purification of materials, especially for the achievement of high purely nano materials. The EIW based purification is mainly suitable for the separation of rarefied gaseous materials in the circumstance of cold atom beam laboratories [7–9].

Theoretical model of atom beam for the material purification is conceptually shown in Fig. 1 (a). Here, we just consider diluted cold atoms where atom-atom interactions could be neglected [10, 11]. Hamiltonian of any individual atom under the coherent propagation field $\mathbf{E}(\mathbf{x}, t) = \hat{e}_z E_0 \cos(\omega t - kx)$ is described in momentum space as [6]

$$\mathbf{H} = \sum_{n=0,1} \varepsilon_n |n\rangle \langle n| + \int dp \frac{p^2}{2M} |p\rangle \langle p| - \frac{\hbar}{2} \int dp (\Omega e^{-i\omega t} |1, p + \hbar k\rangle \langle 0, p| + H.c.), \quad (1)$$

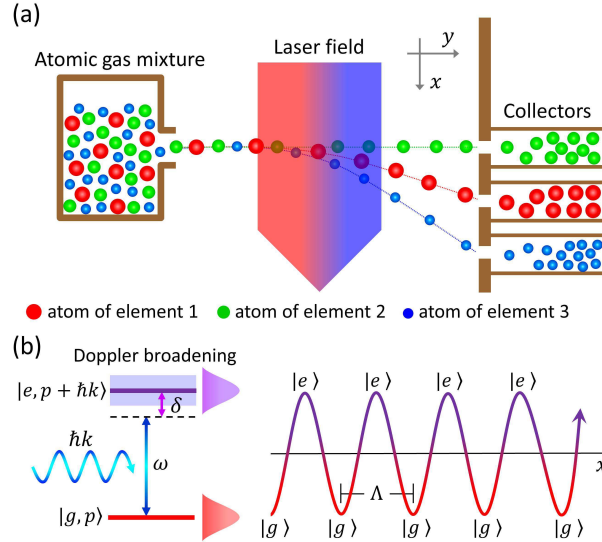


FIG. 1: (Color on line)(a) Schematic illustration of separation and purification. (b)Electromagnetically Induced Walking in the synthetic dimensions of atom.

*Electronic address: wxlai@pku.edu.cn

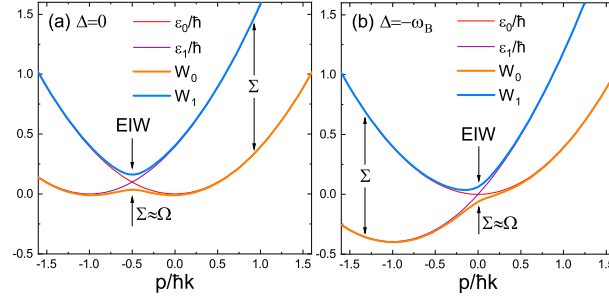


FIG. 2: (Color on line) The position of EIW is shown in the spin-orbit coupled energy structure. (a) Energy gap with the back action shift. (b) The back action shift is removed by the detuning.

where Rabi frequency is $\Omega = |\mu|E_0/\hbar$ with dipole moment of the atom $\mu = \langle 0|e\mathbf{z}|1 \rangle$ [12]. Here, Ω would be taken as real for a definite phase of dipole moment and light. Evolution of the wave function $|\Psi(t)\rangle$ of the atom could be solved through the Schrödinger equation $i\hbar\frac{\partial}{\partial t}|\Psi(t)\rangle = \mathbf{H}|\Psi(t)\rangle$. With the unitary operator $e^{i\mathbf{H}_0 t/\hbar}$, $\mathbf{H}_0 = \varepsilon_0|0\rangle\langle 0| + (\varepsilon_0 + \hbar\omega)|1\rangle\langle 1|$, one can have the Schrödinger equation in interaction picture $i\hbar\frac{\partial}{\partial t}|\varphi(t)\rangle = \mathbf{V}|\varphi(t)\rangle$, where the wave function can be expanded with probability distribution functions as $|\varphi(t)\rangle = \int dp \sum_n \varphi_n(p, t)|n, p\rangle$. V is a time independent Hamiltonian and it can be diagonalized in a subspace of definite momentum p . The eigenfrequencies are $W_{0,1} = \frac{1}{2}(\omega_p + \omega_{p+\hbar k} + \Delta \mp \Sigma)$, in which the transition frequency in interaction picture is $\delta = \omega_p - \omega_{p+\hbar k} - \Delta$ and the atom-light detuning $\Delta = \varepsilon_1 - \varepsilon_0 - \omega$. Fig. 2 (a) and (b) show the eigenfrequencies with the gap $\Sigma = \sqrt{\delta^2 + \Omega^2}$. The energy structure indicates spin-orbit coupling of the neutral atom. Topological chiral edge states and spin-orbit coupling of neutral atom transport can be obtained in optical lattice [13, 14]. The averaged momentum of the atom wave packet can be calculated through the formula $\langle p(t) \rangle = \langle \varphi(t) | p | \varphi(t) \rangle$. From the function of momentum $\langle p(t) \rangle$ we can obtain displacement of the atom $\langle x(t) \rangle = \langle x(0) \rangle + \int_0^t \frac{\langle p(t) \rangle}{M} dt$.

In the strong coupling regime $\Omega \gg \delta$, we have $\Sigma \approx \Omega$ where the EIW would appears as illustrated in Fig. 2. In this regime, the displacement of the atom wave packet has the following simple form

$$\langle x(t) \rangle = \langle x(0) \rangle + \frac{p_c}{M}t + (C_0^2 - C_1^2)\frac{\hbar k}{2M}(t - \frac{\sin(\Omega t)}{\Omega}). \quad (2)$$

Eq.(2) describes the coherent walking of single atoms [6] along the x direction. Then, from the formula of atom wave packet displacement, velocity of the atom in the x direction can be achieved as

$$\langle v(t) \rangle = \frac{p_c}{M} + (C_0^2 - C_1^2)\frac{\hbar k}{2M}(1 - \cos(\Omega t)). \quad (3)$$

It is obvious that displacement and velocity of the atom is changing periodically with the time periodicity $T = \frac{2\pi}{\Omega}$. The averaged velocity in a periodic time $\bar{v} = \frac{1}{T} \int_0^T \langle v(t) \rangle dt$ is

$$\bar{v} = \frac{p_c}{M} + (C_0^2 - C_1^2)\frac{\hbar k}{2M}. \quad (4)$$

Considering the experimental set up in Fig. 1 (a), initial velocity in x coordinate can be zero, $p_c = 0$. In addition, the input atoms are assumed to be in the ground state $C_0 = 1$ now. It results the simple relation between atom velocity and its mass-wave length product as

$$\bar{v} = \frac{h}{2M\lambda}, \quad (5)$$

where h is the Plank constant. Eq.(5) reveals that as soon as the product of atom masses M_i and a resonant wave lengths λ_i of corresponding atoms are different in a mixed atomic gas, $M_i\lambda_i \neq M_j\lambda_j$ for $i \neq j$, these chemical elements could be separated physically in principle.

Samples of chemical elements are listed in table I with related parameters [15]. Every transition considered here is transition between the ground state $|0\rangle$ and an excited state $|1\rangle$. The wavelengths are corresponding to the resonant frequencies of these transitions, respectively. EIW speeds of these atoms are clearly different as shown in this table.

These speed difference gives rise to atom deflection as illustrated in Fig. 1. It is similar to the behavior of magnetic atoms in Stern-Gerlach experiment. The atom displacement in x coordinate can be seen Fig. 3 (a), based on the

TABLE I: Atom samples ($u = 1.67 \times 10^{-27}$ kg)

Element	Mass M (u)	Transition $ 0\rangle \rightarrow 1\rangle$	Wavelength λ (nm)	Speed $\frac{h}{2M\lambda}$ (m/s)
^7Li	7.016004	$2s\ ^2S_{1/2} - 2p\ ^2P_{1/2}^0$	670.7926	0.042153
^{12}C	12.000000	$2s^2 2p^2\ ^3P_0 - 2s^2 2p(^2P^0)3s\ ^3P_1^0$	165.6928	0.099775
^{20}Ne	19.992435	$2p^6\ ^1S_0 - 2p^5(^2P_{1/2}^0)4s\ ^2[1/2]^0$	626.8232	0.01583
^{24}Mg	23.985042	$3s^2\ ^1S_0 - 3s3p\ ^1P_1^0$	285.21251	0.0290
^{25}Mg	24.985837	$3s^2\ ^1S_0 - 3s3p\ ^1P_1^0$	285.21251	0.027838
^{26}Mg	25.982593	$3s^2\ ^1S_0 - 3s3p\ ^1P_1^0$	285.21251	0.02677
^{28}Si	27.976927	$3s^2 3p^2\ ^3P_0 - 3s^2 3p4s\ ^3P_1^0$	251.4316	0.028202
^{40}Ca	39.962591	$4s^2\ ^1S_0 - 4s4p\ ^1P_1^0$	422.6727	0.011745
^{48}Ti	47.947947	$3d^2 4s^2\ a^3F_2 - 3d^2(^3F)4s4p(^3P^0)\ z^3D_1^0$	501.4186	0.0082515
^{56}Fe	55.934939	$3d^6 4s^2\ a^5D_4 - 3d^6(^5D)4s4p(^3P)\ z^5P_3^0$	248.32708	0.014282
^{59}Co	58.933198	$3d^7 4s^2\ a^4F_{9/2} - 3d^7(^4F)4s4p(^3P^0)\ z^4F_{9/2}^0$	352.6850	0.0095446
^{69}Ga	68.925580	$4s^2 4p\ ^2P_{1/2}^0 - 4s^2 5s\ ^2S_{1/2}$	403.2984	0.0071367
^{85}Rb	84.911794	$5s\ ^2S_{1/2} - 5p\ ^2P_{3/2}^0$	780.027	0.0029952
^{87}Rb	86.909187	$5s\ ^2S_{1/2} - 5p\ ^2P_{3/2}^0$	780.027	0.0029264
^{87}Sr	86.908884	$5s^2\ ^1S_0 - 5s5p\ ^1P_1^0$	460.733	0.0049544
^{93}Nb	92.906377	$4d^4\ (a^5D)5s\ a^6D_{1/2} - 4d^3\ 5s(a^5P)5p\ y^6P_{3/2}^0$	353.530	0.0060399
^{107}Ag	106.905092	$4d^{10}\ (^1S)5s^2 S_{1/2} - 4d^{10}\ (^1S)5p\ ^2P_{3/2}^0$	328.0680	0.0056564
^{114}Cd	113.903357	$5s^2\ ^2S_0 - 5s5p\ ^1P_1^0$	228.8022	0.0076122
^{115}In	114.903800	$5p\ ^2P_{1/2}^0 - 6s\ ^2S_{1/2}$	410.17504	0.0042092
^{133}Cs	132.905429	$6s\ ^2S_{1/2} - 6p\ ^2P_{3/2}^0$	852.113	0.0017517
^{153}Eu	152.921225	$4f^7 6s^2\ a^8S_{7/2}^0 - 4f^7(^8S^0)6s6p\ (^1P^0)\ y^8P_{5/2}$	466.188	0.0028011
^{173}Yb	172.938208	$4f^{14}\ (^1S)6s^2\ ^1S_0 - 4f^{14}\ (^1S)6s6p\ ^1P_1^0$	555.6466	0.0020645
^{197}Au	196.966543	$5d^{10} 6s\ ^2S_{1/2} - 5d^{10} 6p\ ^2P_{1/2}^0$	267.5954	0.0037639
^{238}U	238.050784	$5f^3(^4I^0)6d7s^2\ ^5L_6^0 - 5f^3 6d^2 7p\ ^7N_7$	358.48774	0.0023247

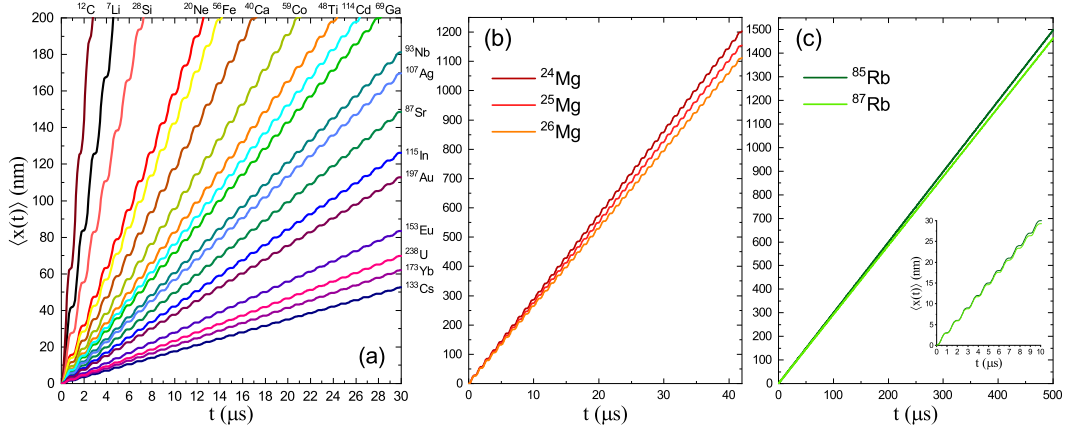


FIG. 3: (Color on line) (a) EIW displacements of different atom samples versus time. (b) EIW displacements of different Magnesium isotopes. (c) EIW displacements of different Rubidium isotopes.

parameters in Table I. Generally, the coherent walking of light atoms move faster and weight atoms move slower. It is good for separation of these atoms. However, due to there are more selections for the resonant wavelengths, some weight atoms can move faster than light atoms, such as ^{114}Cd , light atoms. At the same time, some light atoms may move slower than weight atoms, such as ^{87}Sr . The fact is benefit to the separation of atoms with similar masses, for example, ^{87}Rb and ^{87}Sr , ^{114}Cd and ^{115}In . Atoms plotted in Fig. 3 (a) are easily separated each other. The smallest speed difference comes from speed of ^{173}Yb and speed of ^{238}U . After $30\mu\text{s}$, ^{238}U atom exceeds ^{173}Yb atom nearly 10 nm.

Commonly, isotopes are hardly separated [16]. In the EIW based optical purification, isotopes can be distinguished

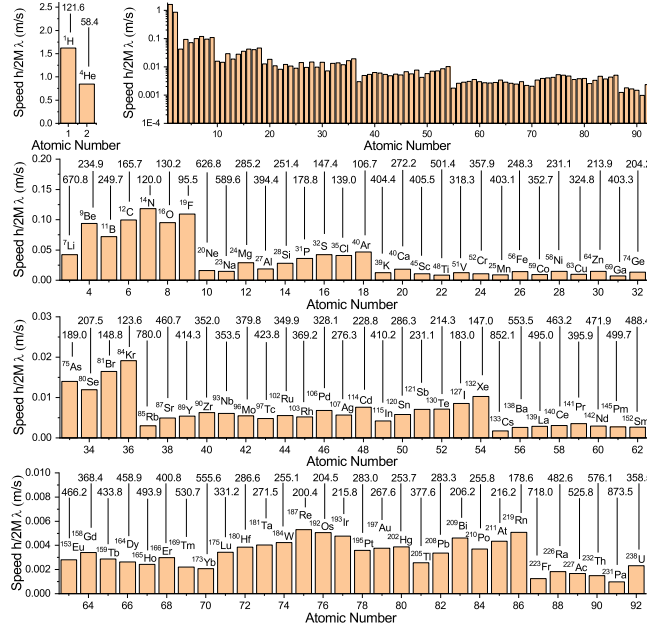


FIG. 4: Velocity-table of chemical elements for given transition wavelengths. Corresponding wavelength with unit nm is written above each element. The inset is total data bars shown below.

only relying on their masses, since energy structure of isotopes are closed to be the same. Isotopes of light atoms are easier to be separated relatively. For example, the Magnesium isotopes shown in Fig. 3 (b). Their distances are nearly 50 nm at time 42 μ s. Wight atoms such as Rubidium isotopes ^{85}Rb and ^{87}Rb leave each other about 50 nm after 500 μ s as illustrated in Fig. 3 (c). The purification ability of the optical method can be further increased by extending coherent time of atoms. This advantage of this method can be seen from Fig. 3 (b) and (c).

A speed table of chemical elements are shown in Fig. 4 for given transition wavelengths. Speeds of atoms appear several clear ladders, from ^1H to ^4He , from ^7Li to ^{19}F , from ^{20}Ne to ^{40}Ar , from ^{39}K to ^{84}Kr , from ^{85}Rb to ^{132}Xe , from ^{133}Cs to ^{219}Rn and from ^{223}Fr to ^{238}U . It is very important for the separation of these chemical elements. Each speed of individual atom can be tuned by selecting other optical transitions.

This optical purification should be developed in molecular materials. It is feasible that cooling and trapping of molecules has been realized recently by many research groups [17–19]. Furthermore, the mass and transition wavelength of these cooled molecules are comparable to the atoms.

In conclusions, we proposed a method of optical purification of materials based on electromagnetically induced waking which is located near the topological edge-state energy in synthetic dimensions of atoms. Properties of this method are determined by difference of mass, difference of optical transition wavelength and coherent time of atom transitions. This method could be mainly used to purify mixed materials which are in the state of fluid or gaseous.

Acknowledgments

This work was supported by the Scientific Research Project of Beijing Municipal Education Commission (BMEC) under Grant No.KM202011232017.

-
- [1] N. De Leon, K. M. Iton, D. Kim, Materials challenges and opportunities for quantum computing hardware. *Science* **372**, 6539 (2021).
 - [2] A. Senichev, Z. O. Martin, S. Peana, D. Sychev, X. Xu, A. S. Lagutchev, A. Boltasseva, V. M. Shalaev, Room-temperature single-photon emitters in silicon nitride. *Sci. Adv.* **7**, 50 (2021).
 - [3] B. Keimer, S. A. Kivelson, M. R. Norman, S. Uchida, J. Zaanen, *Nature* **518**, 179 (2015).
 - [4] Johnpierre Paglione, Richard L. Greene. *Nat. Phys.* **6**, 645 (2010).
 - [5] F. P. G. de Arquer, D. V. Talapin, V. I. Klimov, Y. Arakawa, M. Bayer, E. H. Sargent, Semiconductor quantum dots: Technological progress and future challenges. *Science* **373**, 6555 (2021).

- [6] Wenxi Lai, Electromagnetically Induced Walking. arXiv:2202.04813 [quant-ph] (2022).
- [7] John D. Elgin, Thomas P. Heavner, John Kitching, Elizabeth A. Donley, Jayson Denney, Evan A. Salim, A cold-atom beam clock based on coherent population trapping. *Appl. Phys. Lett.* **115**, 033503 (2019).
- [8] J. M. Kwolek, A. T. Black, Continuous Sub-Doppler-Cooled Atomic Beam Interferometer for Inertial Sensing. *Phys. Rev. Applied* **17**, 024061 (2022).
- [9] S. E. Maxwell, N. Brahms, R. deCarvalho, D. R. Glenn, J. S. Helton, S. V. Nguyen, D. Patterson, J. Petricka, D. DeMille, J. M. Doyle, High-Flux Beam Source for Cold, Slow Atoms or Molecules. *Phys. Rev. Lett.* **95**, 173201 (2005).
- [10] G. L. Gattobigio, A. Couvert, M. Jeppesen, R. Mathevet, D. Guéry-Odelin, *Phys. Rev. A* **80**, 041605 (2009).
- [11] A. Couvert, M. Jeppesen, T. Kawalec, G. Reinaudi, R. Mathevet, D. Guéry-Odelin, *Europhys. Lett.* **83**, 50001 (2008).
- [12] M. O. Scully and M. S. Zubairy, *Quantum Optics*, Cambridge University Press, Cambridge, 1997.
- [13] S. K. Kanungo, J. D. Whalen, Y. Lu, M. Yuan, S. Dasgupta, F. B. Dunning, K. R. A. Hazzard, T. C. Killian, Realizing topological edge states with Rydberg-atom synthetic dimensions. *Nat. Commun.* **13**, 972 (2022).
- [14] L. F. Livi, G. Cappellini, M. Diem, L. Franchi, C. Clivati, M. Frittelli, F. Levi, D. Calonico, J. Catani, M. Inguscio, and L. Fallani, Synthetic Dimensions and Spin-Orbit Coupling with an Optical Clock Transition. *Phys. Rev. Lett.* **117**, 220401 (2016).
- [15] J. E. Sansonettia, W. C. Martin, *Handbook of Basic Atomic Spectroscopic Data*. *J. Phys. Chem. Data* **34**, 1559 (2005).
- [16] Hermann Haken and Hans Christoph Wolf, *The Physics of Atoms and Quanta*, Springer-Verlag, Berlin Heidelberg, 2005.
- [17] E.S. Shuman, J.F. Barry, D. DeMille, Laser cooling of a diatomic molecule. *Nature* **467**, 820 (2010).
- [18] Hyungmok Son, Juliana J. Park, Wolfgang Ketterle, Alan O. Jamison, Collisional cooling of ultracold molecules. *Nature* **580**, 197 (2020).
- [19] Jee Woo Park, Sebastian A. Will, and Martin W. Zwierlein, Ultracold Dipolar Gas of Fermionic $^{23}\text{Na}^{40}\text{K}$ Molecules in Their Absolute Ground State. *Phys. Rev. Lett.* **114**, 205302 (2015).